



Article

HYDroynamics with JETs (HYDJET++): Latest Developments and Results

Garnik Ambaryan, Larissa Bravina, Alexey Chernyshov, Gyulnara Eyyubova, Vladimir Korotkikh, Igor Lokhtin, Sergei Petrushanko, Alexandr Snigirev and Evgeny Zabrodin

Special Issue

Selected Papers from the 13th International Conference on New Frontiers in Physics (ICNFP 2024)





Edited by

Prof. Dr. Larissa Bravina, Prof. Dr. Sonia Kabana and Prof. Dr. Armen Sedrakian



Article

HYDroynamics with JETs (HYDJET++): Latest Developments and Results [†]

Garnik Ambaryan ¹, Larissa Bravina ², Alexey Chernyshov ¹, Gyulnara Eyyubova ³, Vladimir Korotkikh ³, Igor Lokhtin ³ , Sergei Petrushanko ^{3,4} , Alexandr Snigirev ^{3,5}  and Evgeny Zabrodin ^{3,*} 

¹ Physics Department, Lomonosov Moscow State University, RU-119991 Moscow, Russia; metro18g@gmail.com (G.A.); ach1999@yandex.ru (A.C.)

² Department of Physics, University of Oslo, PB 1048 Blindern, N-0316 Oslo, Norway; bravina@fys.uio.no

³ Skobeltsyn Institute of Nuclear Physics, Lomonosov Moscow State University, RU-119991 Moscow, Russia; eyyubova@mail.cern.ch (G.E.); vlk@mail.cern.ch (V.K.); igor@lav01.sinp.msu.ru (I.L.); serguei.petrushanko@cern.ch (S.P.); snig@mail.cern.ch (A.S.)

⁴ Veksler and Baldin Laboratory of High Energy Physics, Joint Institute for Nuclear Research, RU-141980 Dubna, Russia

⁵ Bogoliubov Laboratory of Theoretical Physics, Joint Institute for Nuclear Research, RU-141980 Dubna, Russia

* Correspondence: zabrodin@fys.uio.no

[†] This paper is based on the talk at the 13th International Conference on New Frontiers in Physics (ICNFP 2024), Crete, Greece, 26 August–4 September 2024.

Abstract: Analysis of the (i) charge balance function and (ii) fluctuations of the net electric charge of hadrons in $Pb+Pb$ collisions at center-of-mass energy 2.76 TeV per nucleon pair was performed within a two-component HYDJET++ model. It is shown that neither the widths of the balance function nor the strongly intensive quantities, D and Σ , used to describe the net-charge fluctuations, can be reproduced within the model based on a grand canonical ensemble approach for generating multiparticle production. To solve this problem, it is necessary to take into account exact charge conservation in an event-by-event basis. The corresponding procedure was developed and implemented in the modified HYDJET++ model. It provides a fair description of the experimental data.

Keywords: relativistic heavy-ion collisions; hybrid models; balance function; net-charge fluctuations; canonical charge conservation



Academic Editor: Robert Vertesi

Received: 31 December 2024

Revised: 5 March 2025

Accepted: 26 March 2025

Published: 1 April 2025

Citation: Ambaryan, G.; Bravina, L.; Chernyshov, A.; Eyyubova, G.; Korotkikh, V.; Lokhtin, I.; Petrushanko, S.; Snigirev, A.; Zabrodin, E. HYDroynamics with JETs (HYDJET++): Latest Developments and Results. *Particles* **2025**, *8*, 35. <https://doi.org/10.3390/particles8020035>

Copyright: © 2025 by the authors. Licensee MDPI, Basel, Switzerland. This article is an open access article distributed under the terms and conditions of the Creative Commons Attribution (CC BY) license (<https://creativecommons.org/licenses/by/4.0/>).

1. Introduction

Studies of heavy-ion collisions at relativistic and ultrarelativistic energies carried out at accelerators such as the Super Proton Synchrotron (SPS), $\sqrt{s_{NN}} = 17.3$ GeV, Relativistic Heavy Ion Collider (RHIC), $\sqrt{s_{NN}} = 200$ GeV, and Large Hadron Collider (LHC), $\sqrt{s_{NN}} = 2.76$ TeV and 5.02 TeV, have provided a wealth of information about the properties of dense and hot nuclear matter; see, e.g., [1] and references therein. One of the most important areas of this research is the search for and study of signals associated with the formation of a new state of matter called quark–gluon plasma (QGP).

The signals proposed as indicators of QGP creation are quite diverse. Some of them contain an implicit understanding of the dependence of quark production on time. To accurately determine the formation time of charged particle pairs, a charge balance function (CBF) [2] was proposed. It studies the separation of positively and negatively charged hadrons. Wide CBF widths would indicate early production of charged pairs, while narrow widths would favor the later production of hadrons, characteristic of the hadronization of quark–gluon plasma. Charge balance functions have been studied in various macroscopic and microscopic models, such as the hydrodynamic model [3], hadron resonance gas

(HRG) model [4], coalescence model [5], and so forth [6]. The charge balance function has been also measured in proton–proton (pp), proton/deuteron–nucleus ($p + Pb$ and $d + Au$), and heavy-ion ($Au+Au$ and $Pb+Pb$) collisions at RHIC [7–9] and LHC [10–12] energies. For an extensive review of both theoretical and experimental results, see [13].

Another group of observables, sensitive to the thermodynamic properties and critical behavior of hot and dense media, are event-by-event (EbyE) fluctuations of conserved charges, such as net-baryon or net-electric charges [14,15]. For instance, electric net-charge fluctuations are proportional to the square of the charges in the system, and therefore, they should dramatically decrease in the case of the formation of quark–gluon plasma. To quantify these fluctuations, two new variables, D [16,17] and Σ [18–20], were proposed. In heavy-ion collisions, the net-charge fluctuations were studied at the energies of the SPS [21,22], RHIC [23], and LHC [24,25].

To study these and many other signals of QGP in heavy-ion collisions, one has to rely on the results of model calculations. It is worth mentioning that the majority of these models cannot fairly reproduce, e.g., the centrality dependence of both the charge balance functions and the measures of fluctuations, D and Σ . In the present study, we employed the two-component Monte Carlo HYDJET++ model [26]. Here, the final state represents a superposition of the soft “thermal” and hard states resulting from multiparton fragmentation. We show that in order to adequately describe both the widths of the CBFs and net-charge fluctuations in ultrarelativistic heavy-ion collisions, the model needs further modification.

This paper is organized as follows. Basic features of the default version of the HYDJET++ model are presented in Section 2. Section 3 discusses the charge balance function and its width as a function of centrality and pseudorapidity. The results of the model calculations are compared with the data. Here, we introduce important modifications implemented in the recent version of the HYDJET++ model. In Section 4, the results obtained for the net-charge fluctuations in $Pb+Pb$ collisions at a center-of-mass energy of 2.76 TeV per nucleon pair using the HYDJET++ model are compared with ALICE data [24,25]. Further, the fine-tuning of the model parameters is presented. Conclusions are presented in Section 5.

2. Model Description

Developed for simulating heavy-ion collisions at relativistic and ultrarelativistic energies, the HYDJET++ (HYDroynamics with JETs) model is a Monte Carlo (MC) event generator [26,27] consisting of two parts, describing soft and hard processes, respectively. To describe soft processes, HYDJET++ uses an adapted version of the FASTMC [28,29] model based on the relativistic hydrodynamic parameterization of the chemical and thermal freeze-out hypersurfaces under given freeze-out conditions. The best agreement with experimental data is obtained in the scenario with separated chemical and thermal freeze-out. The simulation of a single event begins with the calculation of the effective volume of the overlap region of colliding nuclei V_{eff} . This volume depends on the average number of participating nucleons, determined from the Glauber multiple scattering model for a given collision centrality, i.e., impact parameter b . The production of particles in the system takes place at the stage of chemical freeze-out according to the prescription of statistical thermal models [30,31]. The composition of hadrons does not change until the stage of thermal freeze-out, after which two- and many-particle decays of resonances occur. HYDJET++ uses an extensive table of resonances, containing more than 360 meson and baryon states, from the statistical model SHARE [32]. At the same time, for the decays of resonances, the HYDJET++ model employs its own original procedure.

In the hard sector, the model considers hard quarks and gluons traversing dense and hot quark–gluon plasma. Here, the PYQUEN (PYTHIA QUENched) [33] model was used,

which takes into account parton energy losses due to gluon emission in the medium and collisional losses due to parton rescattering. The number of jets is generated according to a binomial distribution. Their average number for a heavy-ion collision with some impact parameter b is calculated as a product of the number of binary nucleon–nucleon collisions (NN) and the integral cross-section of the hard process in these collisions with minimal transverse momentum transfer p_T^{min} . This important free parameter of the HYDJET++ model is determined from a comparison with experimental data; see [26]. Partons that were produced in (semi-)hard subprocesses with momentum transfer below the threshold p_T^{min} are removed from the hard-parton spectrum, and their hadronization products are added to the thermalized soft-particle spectra.

This approach, in which hard and soft processes are considered simultaneously within the same model, has proven to be very fruitful. For example, HYDJET++ describes the centrality and transverse momentum dependence of the differential elliptic [34,35] and triangular [36] flow of hadrons in heavy-ion collisions at RHIC and LHC energies, the violation (because of the jets) of the mass hierarchy and the constituent quark scaling (NCQ) of these differential flows at intermediate and high values of p_T [35,37,38], higher harmonics of the anisotropic flow [35,38,39], and their event-by-event fluctuations [40]. As was shown in [41], the model can be modified to take the collisions of deformed nuclei into consideration, such as $Xe+Xe$ at $\sqrt{s_{NN}} = 5.44$ TeV. Further details of the model can be found elsewhere [26,27].

3. Balance Functions of Charged Particles

The charge balance function is defined as follows [2]. Let us denote the number of positive and negative charge particles in a certain pseudorapidity interval $|\eta|$ averaged over all events as $\langle N_+ \rangle$ and $\langle N_- \rangle$, respectively. The average number of unlike-charge pairs with particles separated by the relative pseudorapidity $\Delta\eta = \eta_+ - \eta_-$ is $\langle N_{+-}(\Delta\eta) \rangle$, and similarly for $\langle N_{-+}(\Delta\eta) \rangle$, $\langle N_{++}(\Delta\eta) \rangle$ and $\langle N_{--}(\Delta\eta) \rangle$. Then, the charge balance function as a function of pseudorapidity reads

$$B(\Delta\eta) = \frac{1}{2} \left[\frac{\langle N_{+-}(\Delta\eta) \rangle - \langle N_{++}(\Delta\eta) \rangle}{\langle N_+ \rangle} + \frac{\langle N_{-+}(\Delta\eta) \rangle - \langle N_{--}(\Delta\eta) \rangle}{\langle N_- \rangle} \right]. \tag{1}$$

Similarly, one may introduce the charge balance function $B(\Delta\varphi)$ as a function of the relative azimuthal angle $\Delta\varphi$. The width of the pseudorapidity interval depends on the detector parameters. For instance, the ALICE Collaboration used the pseudorapidity interval $|\eta| < 0.8$ in the analysis, and each term $N(\Delta\eta)$ was corrected for the acceptance limitation [11]. The width of the balance function distribution is defined as

$$\langle \Delta\eta \rangle = \sum_{i=1}^j [B(\Delta\eta_i) \cdot \Delta\eta_i] / \sum_{i=1}^j B(\Delta\eta_i), \tag{2}$$

where $B(\Delta\eta_i)$ denotes the balance function value for each bin $\Delta\eta_i$, and the sum runs over all j bins.

The charge balance function dependence on the pseudorapidity $\Delta\eta$ calculated in the HYDJET++ model for $Pb+Pb$ collisions at the center-of-mass energy per nucleon pair $\sqrt{s_{NN}} = 2.76$ TeV with centrality 0–5%, 20–30%, and 50–60% is shown in Figure 1. One can see that all three distributions have similar widths despite the different contributions of the soft and hard processes to the total particle spectrum in central (0–5%) and peripheral (50–60%) collisions. It is worth noting that the transverse momentum range of the studied

hadrons, $0.3 < p_T < 1.5 \text{ GeV}/c$, is the same as that chosen for ALICE analysis in [11]. This means that the majority of particles comes from the soft processes and that the width of the charge balance function in these processes in the HYDJET++ model does not depend on the centrality of nuclear collision. Before the detailed analysis of the sources of particle correlations in HYDJET++, let us compare the widths of the CBFs measured by the ALICE Collaboration [10] in the following intervals with the calculations:

- (1) $2.0 < p_{T, \text{assoc}} < 3.0 < p_{T, \text{trig}} < 4.0 \text{ GeV}/c$ and
- (2) $3.0 < p_{T, \text{assoc}} < 8.0 < p_{T, \text{trig}} < 15.0 \text{ GeV}/c$

In line with the experimental procedure, the widths were calculated not in the entire intervals of $\Delta\eta$ and $\Delta\phi$, but in the narrow interval. The balance function distributions were fitted to the sum of a Gaussian and a constant, and the final width is calculated within $3\sigma_{\text{Gauss}}$.

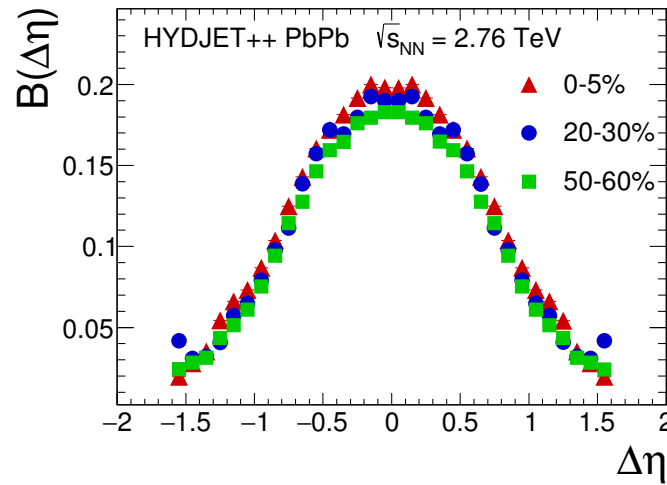


Figure 1. Balance function $B(\Delta\eta)$ of charged hadrons in HYDJET++-calculated $Pb+Pb$ collisions at $\sqrt{s_{NN}} = 2.76 \text{ TeV}$ for centrality bins: (i) 0–5% (red triangles), (ii) 20–30% (blue circles), and (iii) 50–60% (green squares).

The comparison is displayed in Figure 2. We see that the widths of the balance functions for hadrons from the two selected intervals are practically independent of the collision centrality. For the first p_T -interval, the model predicts narrower distributions, while for the interval with higher transverse momentum values, the agreement with experimental data is good. But in this range, the hard processes, i.e., jets, dominate the particle production, whereas the contribution of the soft processes is very weak. Unlike-sign charges decoupled from jets are correlated because of the exact charge conservation during the jet fragmentation. Note also that hadrons with higher transverse momenta are created at earlier stages of the parton cascade. Here, the charge correlations are stronger, and this circumstance explains the decrease in the width of the balance functions with an increasing p_T interval.

In the soft sector, the HYDJET++ model employs the statistical model for particle production. In the framework of grand canonical formalism, all primary particles, hereinafter called direct, are generated independently, implying that there are no balancing correlations between the oppositely charged hadrons. Therefore, the only source of correlations in phase space between final-state particles are decays in hadronic resonances. This is not enough to describe the balance functions of charged particles. The following question arises: is it possible to take into account the pair production of charged particles and, accordingly, the correlations between them within the framework of a statistical model? An elegant solution to this problem was proposed in [42].

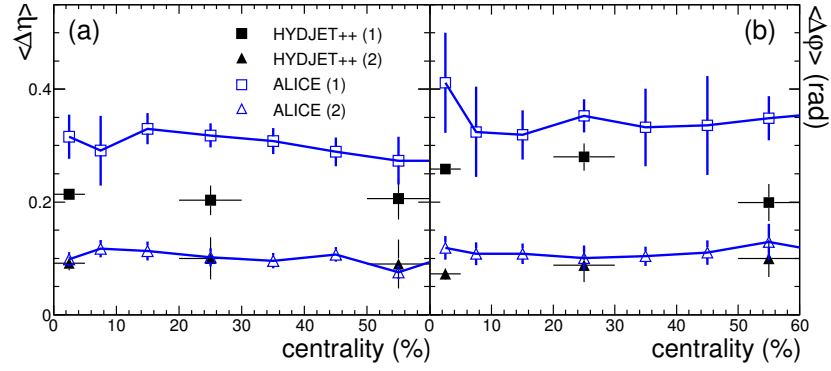


Figure 2. (a) Centrality dependence of the width of the balance function of charged hadrons as a function of pseudorapidity in $Pb+Pb$ collisions at $\sqrt{s_{NN}} = 2.76$ TeV. The correlations are studied in two p_T intervals, indicated as (1) and (2) (see text). For interval (1), HYDJET++ calculations and the data from [11] are represented as full and open squares, respectively, whereas for interval (2), the calculations and the data are represented as full and open triangles. Lines are drawn to guide the eye. (b) The same as (a) but for the width of the balance function as a function of the relative angle $\Delta\phi$.

Let us consider the case of electrically neutral matter with zero net charge. This situation is relevant for the midrapidity range in heavy-ion collisions at RHIC and LHC energies. Generalization to non-zero net electric charge will be discussed also. As a first step, all soft-component hadrons are still generated according to the grand canonical ensemble prescription, i.e., the charges of different signs are uncorrelated. Then, half of the charged hadrons are randomly removed from the particle spectrum. The Monte Carlo implementation of this procedure assumes that each directly produced charged hadron is either discarded with probability 50% or remains untouched. After that, for each of the remaining hadrons, its counterpart with opposite electric charge and similar transverse momentum is generated. As was shown in [42], the charged particle spectra in pseudorapidity, angular, and transverse momentum, generated within the standard and modified approaches, are practically identical for the statistics of 1000 events and more. The particles produced in this way have an azimuthal angle ϕ_2 and rapidity η_2 , which are distributed in accordance with the normal Gaussian distribution around the azimuthal angle ϕ_1 and rapidity η_1 of the original hadron:

$$P_{\mu,\sigma}(x) = \frac{1}{\sqrt{2\pi}\sigma} \exp \left[-\frac{(x - \mu)^2}{2\sigma^2} \right], \quad (3)$$

where $x = (\eta_2, \phi_2)$, $\mu = (\eta_1, \phi_1)$, and $\sigma = (\sigma_\eta, \sigma_\phi)$. We see that the strength of the charge correlations of the produced hadrons is determined by the values of the dispersions, σ_η and σ_ϕ . These dispersions are new centrality-dependent free parameters of the modified HYDJET++ whose values can be fixed through comparisons with the existing experimental data at a certain centrality. The presented scheme can be extended to a matter with unbalanced electric charges. Here, it is necessary to randomly select the number of hadrons corresponding to the excess charge and keep it untouched. The above procedure should then be applied for the rest of the particle spectrum.

The comparison of the modified model calculations with the default ones and the data is shown in Figure 3. It can be seen that the calculations within the modified model well reproduce the experimentally observed dependencies of the balance function widths on centrality. For this, it is necessary that the dispersions of the Gaussian distributions increase with the growth of the impact parameter. This circumstance indicates that the charge correlations of direct hadrons weaken when moving from central collisions to more peripheral ones. This can be explained as follows. In the HYDJET++ model, as in other statistical and hydrodynamic models, all particles are produced at the moment of chemical freeze-out. Part of the information about the early stage of the system's evolution is encoded

in these models in the parameters of the soft hadron radiation sources. In particular, the charge correlations of hadrons are encoded using the dispersions of the Gaussian distributions. In the case of central collisions of heavy ions, the number of independent particle sources in which the charge is exactly conserved is quite large. As the impact parameter increases, the number of independent particle sources decreases, and as a consequence, fluctuations increase. These fluctuations reduce the magnitude of the charge correlations, which leads to an increase in the dispersions of both distributions for more peripheral collisions.

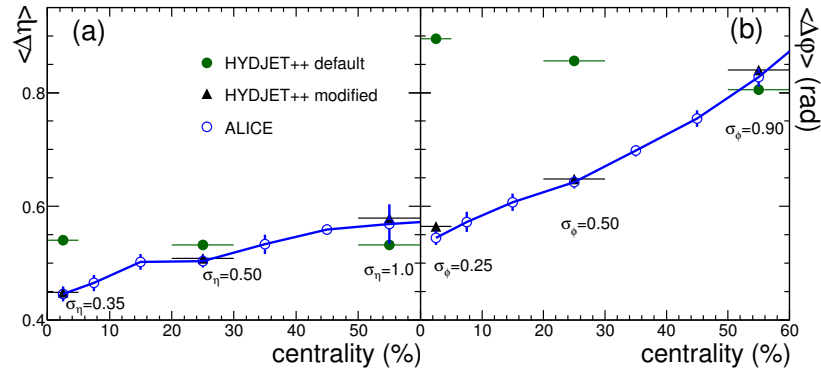


Figure 3. (a) Centrality dependence of the width of the balance function of charged hadrons as a function of pseudorapidity in $Pb+Pb$ collisions at $\sqrt{s_{NN}} = 2.76$ TeV. The correlations are studied within the HYDJET++-default (full green circles) and HYDJET++-modified (full blue triangles) models. ALICE data from [11] are indicated as blue open circles. Lines are drawn to guide the eye. (b) The same as (a) but for the width of the balance function as a function of the relative angle $\Delta\phi$.

Is it possible to avoid fitting the dispersion value at each centrality? It turns out that the answer is yes. As was shown in [43], the fluctuation centrality dependence of the dispersions can be represented as

$$\sigma_x(C) = \sigma_x(C_0) \sqrt{\frac{1 - C_0^{1/2}}{1 - C^{1/2}}} \quad (4)$$

where the dispersion $\sigma_x(C_0)$ is determined for the most central collisions C_0 . In the case under consideration, these values will be $C_0 = 0$ and $\sigma_{\eta}(0) = 0.35$, respectively. The dispersion values calculated with Formula (4) turn out to be very close to the fitting values, as shown in Figure 3. Thus, it is possible to skip the procedure of fitting new free parameters of the model in each centrality bin and use a simple fluctuation formula given by Equation (4).

4. Net-Charge Fluctuations

Let us denote the total number of charged particles in a relativistic heavy-ion collision as $N_{ch} = N_+ + N_-$, the net charge as $Q = N_+ - N_-$, and the ratio of positive to negative charges as $R = \frac{N_+}{N_-}$. In assuming that $\langle N_{ch} \rangle \gg \langle Q \rangle$, it is possible to show [16] that the variances $\langle \delta R^2 \rangle$ and $\langle \delta Q^2 \rangle$ are linked via

$$\langle N_{ch} \rangle \langle \delta R^2 \rangle = 4 \frac{\langle \delta Q^2 \rangle}{\langle N_{ch} \rangle} = D \quad (5)$$

Parameter D emerging in Equation (5) is the final observable measure [14,16]. It is related to the event-by-event fluctuations via the variable $\nu_{+-,\text{dyn}}$, which is the difference between the relative charged particle multiplicities and statistical fluctuations [15]:

$$D = \langle N_{ch} \rangle \nu_{+-,\text{dyn}} + 4, \tag{6}$$

where

$$\nu_{+-,\text{dyn}} = \frac{\langle N_+^2 \rangle - \langle N_+ \rangle^2}{\langle N_+ \rangle^2} + \frac{\langle N_-^2 \rangle - \langle N_- \rangle^2}{\langle N_- \rangle^2} - 2 \frac{\langle N_+ N_- \rangle}{\langle N_+ \rangle \langle N_- \rangle}. \tag{7}$$

Another measure of particle multiplicity correlations and fluctuations, $\Sigma[N_+, N_-]$, was introduced in [18]. It is also related to $\nu_{+-,\text{dyn}}$ as

$$\frac{\langle N_+ \rangle + \langle N_- \rangle}{\langle N_+ \rangle \langle N_- \rangle} (\Sigma[N_+, N_-] - 1) = \nu_{+-,\text{dyn}}. \tag{8}$$

Both D and $\Sigma[N_+, N_-]$ are strongly intensive quantities, i.e., they do not depend on both the volume and volume fluctuations of the system. Note also that under the assumption of charge balance in the pseudorapidity window, $\Sigma[N_+, N_-]$ is linked to the balance function $B(\Delta\eta)$ through the integral of the latter [44]:

$$\Sigma[N_+, N_-] = 1 - \int B(\Delta\eta) d\Delta\eta. \tag{9}$$

Last but not least, the predictions for the fluctuation magnitudes were obtained within the grand canonical ensemble. Here, the charge is conserved on average. To take into account the particle correlations caused by canonical charge conservation, corrections for the global charge conservation of $\nu_{(+,-,\text{dyn})}$ are needed. One of the possible corrections was proposed in [17]:

$$\nu_{+-,\text{dyn}}^{\text{corr}} = \nu_{+-,\text{dyn}} + \frac{4}{\langle N_{tot} \rangle}, \tag{10}$$

where $\langle N_{tot} \rangle$ is the total charged multiplicity in full phase space.

As noted above, the HYDJET++ model uses the grand canonical ensemble approximation to describe soft hadron production. In this case, hadron production on the freeze-out hypersurface corresponds to particle emission by independent sources, and no corrections for global charge conservation are needed. Thus, one might expect the values of D and Σ to be close to those predicted for the ideal hadron gas model, i.e., $D = 4$ and $\Sigma = 1$. Figure 4a shows that D is indeed close to 4 for directly produced hadrons. Resonance decays lead to a decrease in D to about 3. The smallest D values are observed for hadrons produced by jet fragmentation, since the correlations of charged hadrons in jets are even stronger than for resonances. Because of the exact charge conservation of hadrons in jets, the hard component of HYDJET++ in Figure 4a was corrected to take into account global charge conservation; see Equation (10). This correction is more pronounced for larger phase spaces.

In contrast, the HYDJET++ model with the modifications used to describe the width of the charge balance functions significantly reduces the values of D , as can be seen in Figure 4b. Interestingly, in this case, the charge correlations of direct hadrons predict the smallest value of D , and the resonance decays weaken the correlations, thereby increasing the value of D . A similar effect from the decay of resonances in the final state can also influence the fluctuations in the quark–gluon plasma. Another process that increases the magnitude of fluctuations for the QGP is the contribution of partially thermalized hard minijets, which are still present in the considered range of relatively low transverse momenta p_T , $0.2 < p_T < 5 \text{ GeV}/c$. These circumstances may help to understand why the measured experimentally corrected values of D turn out to be higher than those predicted for QGP.

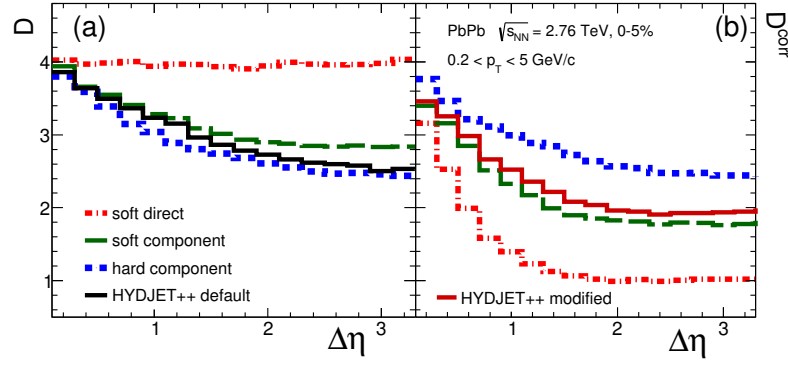


Figure 4. D and D^{corr} represented as a function of the $\Delta\eta$. (a) D represented as a function of the $\Delta\eta$ window for $Pb+Pb$ collisions generated in the HYDJET++ calculations in default mode at $\sqrt{s_{NN}} = 2.76$ TeV with centrality of 0–5% for direct soft hadrons (red dash-dotted line), hard processes (blue dashed line), soft processes (green dashed line), and the resulting total value (full black line); (b) the same as (a) but for D^{corr} in modified model calculations.

Figure 5a displays a comparison of the experimental data of $D^{corr}(\Delta\eta)$ in central 0–5% collisions of $Pb+Pb$ at $\sqrt{s_{NN}} = 2.76$ TeV, measured by the ALICE Collaboration [24], with the calculations of the AMPT [45], HIJING [46], and HYDJET++ models. The range of transverse momenta $0.2 < p_T < 5$ GeV/c, similarly to the ALICE data, was used in the calculations. In this case, the predictions of the HIJING and modified HYDJET++ models were corrected for global charge conservation, while the predictions of the AMPT and default HYDJET++ models were not corrected, since in them, the global electric charge is not conserved, in general, in each individual event. A comparison of the model results with the experimental values of $\Sigma - 1$ obtained by ALICE for central 0–5% $Pb+Pb$ collisions at $\sqrt{s_{NN}} = 5.02$ TeV [25] is presented in Figure 5b. The range of transverse momenta of hadrons is the same as that at lower energy.

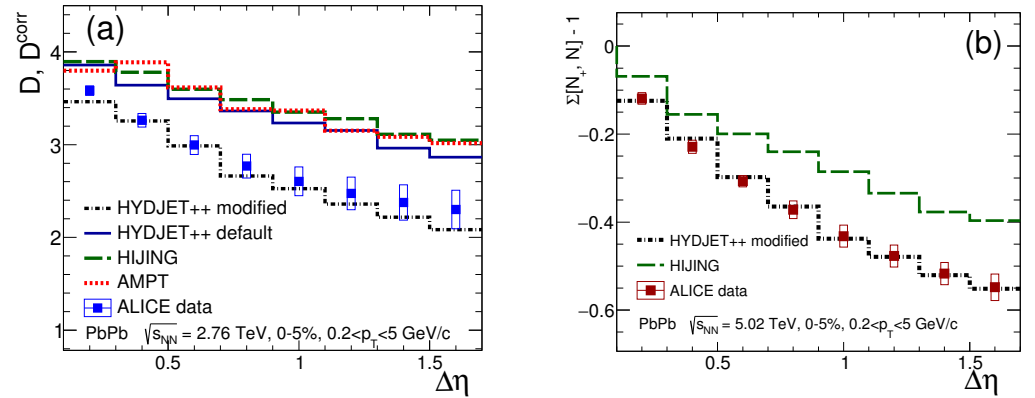


Figure 5. (a) D (for AMPT and default HYDJET++) and D^{corr} (for HIJING and modified HYDJET++) represented as a function of the $\Delta\eta$ window for the HYDJET++ default (full blue histogram), HYDJET++ modified (black dash-dotted line), AMPT (red dotted line), and HIJING (green dashed line) models for the $Pb+Pb$ at 2.76 TeV with centrality of 0–5%, in comparison with the ALICE data (blue squares) from [24]; (b) $\Sigma[N_+, N_-] - 1$ as a function of $\Delta\eta$ for HYDJET++ modified (black dash-dotted histogram) and HIJING (green dashed line) models for the $Pb+Pb$ at 5.02 TeV with centrality of 0–5% in comparison with the ALICE data (brown squares) extracted from [25].

One can see that, unlike the other models, the modified HYDJET++ model well reproduces the dependencies of both D^{corr} and $\Sigma - 1$ on $\Delta\eta$. For a more accurate quantitative description of the dependencies of both measures of fluctuations on centrality, however, the strength of pairwise correlations in the model should be slightly reduced. The point is that in the previous section, the strength of pairwise correlations was adjusted to describe

the widths of the balance functions. Since the measures D and Σ are related to the integral of the balance function, where both the width and amplitude of the latter are important, additional adjustment of the model parameters is necessary [44]. The dispersion σ_η from Equation (3) was increased from 0.35 to 0.5 for centrality 0–5%, from 0.5 to 0.7 for centrality 20–30%, and from 1.0 to 1.1 for centrality 50–60%.

The dependence of the measured values of the variables D and $\Sigma - 1$ on the centrality in $Pb+Pb$ collisions at $\sqrt{s_{NN}} = 2.76$ TeV was investigated experimentally [24] as a function of $\langle N_{part} \rangle$ and $\langle dN_{ch}/d\eta \rangle$, respectively. These data are shown in Figure 6a,b, together with the results of calculations performed with the previous and new set of tuned parameters in the HYDJET++ model for three centralities, 0–5%, 20–30%, and 50–60%. The pseudorapidity windows were chosen to be symmetric about the midrapidity, $\eta = 0$. As can be seen from these figures, the HYDJET++ model with the new settings better reproduces the experimental data for both D^{corr} and $\Sigma[N_+, N_-] - 1$. We also checked that deviations in the widths of charge balance functions obtained in calculations with the new tuned parameters from those provided in Section 3 are within 7% accuracy.

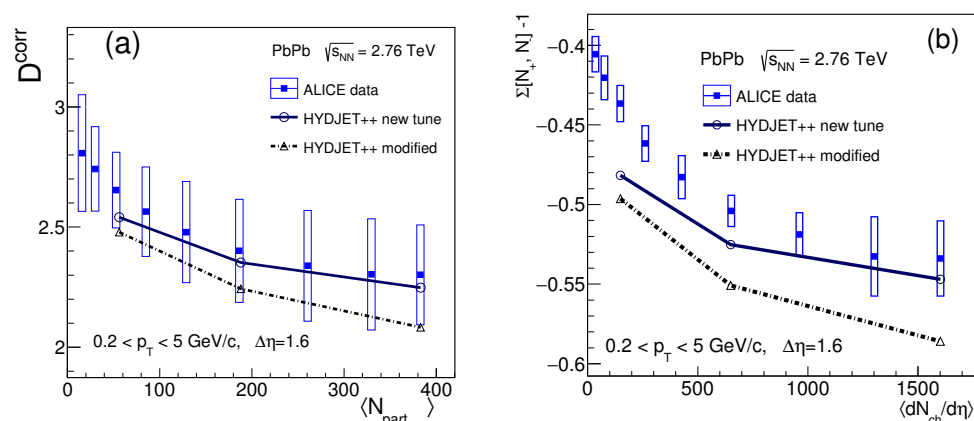


Figure 6. (a) D^{corr} represented as a function of N_{part} for the HYDJET++-modified (open triangles) and newly tuned HYDJET++ (open circles) model calculations of $Pb+Pb$ at 2.76 TeV in comparison with ALICE data (full squares) extracted from [24]. The lines are drawn to guide the eye. (b) The same as (a) but for $\Sigma[N_+, N_-] - 1$ represented as a function of $dN_{ch}/d\eta$.

5. Conclusions

We present here a further important modification of the two-component HYDJET++ model. The need to introduce these changes into the model arose from the analysis of the (i) charge balance function and (ii) fluctuations of the net electric charge of hadrons in lead–lead collisions at a center-of-mass energy of 2.76 TeV and 5.02 TeV per nucleon pair used in HYDJET++.

It is shown that the main shortcoming of macroscopic statistical models when it comes to reproducing such data is the use of a grand canonical ensemble to describe multiparticle production. In this approach, the net electric charge is conserved on average, and hadrons with unlike-sign charges are uncorrelated. Correlations due to final-state interactions, such as decays of resonances, and correlations of hadrons decoupling from jets are insufficient to describe the experimental data. To solve this problem, it is necessary to take into account the pair production of hadrons of opposite sign in every single event.

A proper qualitative and quantitative description of both the charge balance function and the net electric charge fluctuations in this energy range implies a modification of the basic (or default) model by explicitly incorporating charge conservation into the statistical approach. This procedure was developed and first introduced into Monte Carlo event

generators of this kind. The presented algorithm can be implemented in any other models using statistical hadronization.

Author Contributions: All authors contributed equally to this work. All authors have read and agreed to the published version of the manuscript.

Funding: A.C. acknowledges support from the BASIS Foundation under grant No. 23-2-10-2-1.

Data Availability Statement: The data presented in this study are available on request from the corresponding author.

Acknowledgments: Fruitful discussions with A.I. Demianov are gratefully acknowledged.

Conflicts of Interest: The authors declare no conflicts of interests.

References

- Harris, J.W.; Muller, B. "QGP Signatures" Revisited. *Eur. Phys. C* **2024**, *84*, 247.
- Bass, S.A.; Danielewicz, P.; Pratt, S. Cloning hadronization in relativistic heavy ion collisions with balance functions. *Phys. Rev. Lett.* **2000**, *85*, 2689. [[PubMed](#)]
- Ling, B.; Springer, T.; Stephanov, M. Hydrodynamics of charge fluctuations and balance functions. *Phys. Rev. C* **2014**, *89*, 064901.
- Florkowski, W.; Broniowski, W.; Bozek, P. Production of resonances in a thermal model: Invariant mass spectra and balance functions. *J. Phys. G* **2004**, *30*, S1321.
- Bialas, A. Balance functions in coalescence model. *Phys. Lett. B* **2004**, *579*, 31. [[CrossRef](#)]
- Cheng, S.; Petriconi, S.; Pratt, S.; Skoby, M.; Gale, C.; Jeon, S.; Topor, Pop, V.; Zhang, Q.H. Statistical and dynamic models of charge balance functions. *Phys. Rev. C* **2004**, *69*, 054906.
- STAR Collaboration. Narrowing of the balance function with centrality in Au+Au collisions at $\sqrt{s_{NN}} = 130$ GeV. *Phys. Rev. Lett.* **2003**, *90*, 172301.
- STAR Collaboration. Balance Functions from Au+Au, d+Au, and p+p Collisions at $\sqrt{s_{NN}} = 200$ GeV. *Phys. Rev. C* **2010**, *82*, 024905.
- STAR Collaboration. Beam-energy dependence of charge balance functions from Au+Au collisions at energies available at the BNL Relativistic Heavy Ion Collider. *Phys. Rev. C* **2016**, *94*, 024909.
- ALICE Collaboration. Multiplicity and transverse momentum evolution of charge-dependent correlations in pp, p-Pb, and Pb-Pb collisions at the LHC. *Eur. Phys. J. C* **2016**, *76*, 86.
- ALICE Collaboration. Charge correlations using the balance function in Pb-Pb collisions at $\sqrt{s_{NN}} = 2.76$ TeV. *Phys. Lett. B* **2013**, *723*, 267. [[CrossRef](#)]
- Pan, J. Balance functions of charged hadron pairs $(\pi, K, p) \otimes (\pi, K, p)$ in Pb-Pb collisions at $\sqrt{s_{NN}} = 2.76$ TeV. *Nucl. Phys. A* **2019**, *982*, 315.
- Tawfik, A.; Shalaby, A.G. Balance Function in High-Energy Collisions. *Adv. High Energy Phys.* **2015**, *2015*, 186812.
- Asakawa, M.; Heinz, U.; Muller, B. Fluctuation probes of quark deconfinement. *Phys. Rev. Lett.* **2000**, *85*, 2072. [[CrossRef](#)]
- Jeon, S.; Koch, V. Event by event fluctuations. In *Quark-Gluon Plasma 3*; Hwa, R., Wang, X.-N., Eds.; World Scientific: Singapore, 2004; p. 430.
- Jeon, S.; Koch, V. Charged particle ratio fluctuation as a signal for QGP. *Phys. Rev. Lett.* **2000**, *85*, 2076.
- Pruneau, C.; Gavin, S.; Voloshin, S. Methods for the study of particle production fluctuations. *Phys. Rev. C* **2002**, *66*, 044904.
- Gorenstein, M.I.; Gazdzicki, M. Strongly Intensive Quantities. *Phys. Rev. C* **2011**, *84*, 014904. [[CrossRef](#)]
- Gazdzicki, M.; Gorenstein, M.I.; Mackowiak-Pawlowska, M. Normalization of strongly intensive quantities. *Phys. Rev. C* **2013**, *88*, 024907. [[CrossRef](#)]
- Wu, X.; Ren, Y.; Zhang, J.; Xu, Z.; Wei, D.; Hua, L.; Zhang, C.; Huo, L. Analysis of strongly intensive quantities for event-by-event transverse momentum and multiplicity fluctuations using the AMPT model. *J. Phys. G* **2021**, *48*, 105101. [[CrossRef](#)]
- NA49 Collaboration. Measurement of event-by-event transverse momentum and multiplicity fluctuations using strongly intensive measures $\Delta[P_T, N]$ and $\Sigma[P_T, N]$ in nucleus-nucleus collisions at the CERN Super Proton Synchrotron. *Phys. Rev. C* **2015**, *92*, 044905.
- NA61/SHINE Collaboration. Multiplicity and transverse momentum fluctuations in inelastic proton-proton interactions at the CERN Super Proton Synchrotron. *Eur. Phys. J. C* **2016**, *76*, 635.
- STAR Collaboration. Beam-Energy and System-Size Dependence of Dynamical Net Charge Fluctuations. *Phys. Rev. C* **2009**, *79*, 024906.
- ALICE Collaboration. Net-Charge Fluctuations in Pb-Pb collisions at $\sqrt{s_{NN}} = 2.76$ TeV. *Phys. Rev. Lett.* **2013**, *110*, 152301. [[CrossRef](#)]
- Khan, S. Measurements of net-charge fluctuations across various colliding systems with ALICE. In Proceedings of the European Physics Society conference on High Energy Physics 2021, Online, 26–30 July 2021; p. 319.

26. Lokhtin, I.P.; Malinina, L.V.; Petrushanko, S.V.; Snigirev, A.M.; Arsene, I.; Tywoniuk, K. Heavy ion event generator HYDJET++ (HYDrodynamics plus JETs). *Comput. Phys. Commun.* **2009**, *180*, 779.
27. Lokhtin, I.P.; Belyaev, A.V.; Malinina, L.V.; Petrushanko, S.V.; Rogochaya, E.P.; Snigirev, A.M. Hadron spectra, flow and correlations in PbPb collisions at the LHC: Interplay between soft and hard physics. *Eur. Phys. J. C* **2012**, *72*, 2045.
28. Amelin, N.S.; Lednicky, R.; Pocheptsov, T.A.; Lokhtin, I.P.; Malinina, L.V.; Snigirev, A.M.; Karpenko, I.A.; Sinyukov, Y.M. A Fast hadron freeze-out generator. *Phys. Rev. C* **2006**, *74*, 064901. [[CrossRef](#)]
29. Amelin, N.S.; Lednicky, R.; Lokhtin, I.P.; Malinina, L.V.; Snigirev, A.M.; Karpenko, I.A.; Sinyukov, Y.M.; Arsene, I.; Bravina, L. Fast hadron freeze-out generator. Part II. Noncentral collisions. *Phys. Rev. C* **2008**, *77*, 014903.
30. Cleymans, J.; Oeschler, H.; Redlich, K.; Wheaton, S. Comparison of chemical freeze-out criteria in heavy-ion collisions. *Phys. Rev. C* **2006**, *73*, 034905.
31. Andronic, A.; Braun-Munzinger, P.; Stachel, J. Thermal hadron production in relativistic nuclear collisions. *Acta Phys. Polon. B* **2009**, *40*, 1005.
32. Torrieri, G.; Steinke, S.; Broniowski, W.; Florkowski, W.; Letessier, J.; Rafelski, J. SHARE: Statistical hadronization with resonances. *Comput. Phys. Commun.* **2005**, *167*, 229. [[CrossRef](#)]
33. Lokhtin, I.P.; Snigirev, A.M. A Model of jet quenching in ultrarelativistic heavy ion collisions and high-p(T) hadron spectra at RHIC. *Eur. Phys. J. C* **2006**, *45*, 211. [[CrossRef](#)]
34. Eyyubova, G.; Bravina, L.V.; Zabrodin, E.; Korotkikh, V.L.; Lokhtin, I.P.; Malinina, L.V.; Petrushanko, S.V.; Snigirev, A.M. Jets and decays of resonances: Two mechanisms responsible for reduction of elliptic flow at the CERN Large Hadron Collider (LHC) and restoration of constituent quark scaling. *Phys. Rev. C* **2009**, *80*, 064907.
35. Bravina, L.V.; Brusheim, J.B.H.; Eyyubova, G.K.; Korotkikh, V.L.; Lokhtin, I.P.; Malinina, L.V.; Petrushanko, S.V.; Snigirev, A.M.; Zabrodin, E.E. Higher harmonics of azimuthal anisotropy in relativistic heavy ion collisions in HYDJET++ model. *Eur. Phys. J. C* **2014**, *74*, 2807.
36. Crkovska, J.; Bielčík, J.; Bravina, L.; Johansson, B.B.; Zabrodin, E.; Eyyubova, G.; Korotkikh, V.L.; Lokhtin, I.P.; Malinina, L.V.; Petrushanko, S.V.; et al. Influence of jets and decays of resonances on the triangular flow in ultrarelativistic heavy-ion collisions. *Phys. Rev. C* **2017**, *95*, 014910.
37. Zabrodin, E.E.; Bravina, L.V.; Eyyubova, G.K.; Lokhtin, I.P.; Malinina, L.V.; Petrushanko, S.V.; Snigirev, A.M. Influence of jets and resonance decays on the constituent quark scaling of elliptic flow. *J. Phys. G* **2010**, *37*, 094060.
38. Bravina, L.; Johansson, B.B.; Zabrodin, E.E.; Eyyubova, G.; Korotkikh, V.L.; Lokhtin, I.P.; Malinina, L.V.; Petrushanko, S.V.; Snigirev, A.M. Hexagonal flow v_6 as a superposition of elliptic v_2 and triangular v_3 flows. *Phys. Rev. C* **2014**, *89*, 024909.
39. Eyyubova, G.; Korotkikh, V.L.; Lokhtin, I.P.; Petrushanko, S.V.; Snigirev, A.M.; Bravina, L.; Zabrodin, E.E. Angular dihadron correlations as an interplay between elliptic and triangular flows. *Phys. Rev. C* **2015**, *91*, 064907.
40. Bravina, L.V.; Fotina, E.S.; Korotkikh, V.L.; Lokhtin, I.P.; Malinina, L.V.; Nazarova, E.N.; Petrushanko, S.V.; Snigirev, A.M.; Zabrodin, E.E. Anisotropic flow fluctuations in hydro-inspired freeze-out model for relativistic heavy ion collisions. *Eur. Phys. J. C* **2015**, *75*, 588.
41. Pandey, S.; Singh, B.K. Transverse momentum spectra and suppression of charged hadrons in deformed Xe+Xe collisions at $\sqrt{s_{NN}} = 5.44$ TeV using HYDJET++ model. *Eur. Phys. J. A* **2023**, *59*, 6.
42. Chernyshov, A.S.; Eyyubova, G.K.; Korotkikh, V.L.; Lokhtin, I.P.; Malinina, L.V.; Petrushanko, S.V.; Snigirev, A.M.; Zabrodin, E.E. Toward a description of the centrality dependence of the charge balance function in the HYDJET++ model. *Chin. Phys. C* **2023**, *47*, 084107.
43. Eyyubova, G.; Korotkikh, V.L.; Snigirev, A.M.; Zabrodin, E.E. Eccentricities, fluctuations and A-dependence of elliptic and triangular flows in heavy-ion collisions. *J. Phys. G* **2021**, *48*, 095101. [[CrossRef](#)]
44. Ambaryan, G.O.; Chernyshov, A.S.; Eyyubova, G.K.; Korotkikh, V.L.; Lokhtin, I.P.; Petrushanko, S.V.; Snigirev, A.M.; Zabrodin, E.E. Modeling net-charge fluctuations in heavy-ion collisions at the LHC. *Chin. Phys. C* **2025**, *49*, 014109. [[CrossRef](#)]
45. Lin, Z.W.; Ko, C.M.; Li, B.A.; Zhang, B.; Pal, S. A Multi-phase transport model for relativistic heavy ion collisions. *Phys. Rev. C* **2005**, *72*, 064901. [[CrossRef](#)]
46. Gyulassy, M.; Wang, X.-N. HIJING 1.0: A Monte Carlo program for parton and particle production in high-energy hadronic and nuclear collisions. *Comput. Phys. Commun.* **1994**, *83*, 307.

Disclaimer/Publisher’s Note: The statements, opinions and data contained in all publications are solely those of the individual author(s) and contributor(s) and not of MDPI and/or the editor(s). MDPI and/or the editor(s) disclaim responsibility for any injury to people or property resulting from any ideas, methods, instructions or products referred to in the content.